Predictions of V_{RF} on a Langmuir probe under the RF heating spiral on the divertor floor on NSTX-U*

J.C. Hosea[1], R.J. Perkins[1], M.A. Jaworski[1], G.J. Kramer[1], J-W Ahn[2], R.E. Bell[1], N. Bertelli[1], S. Gerhardt[1], T.K. Gray[2], B.P. LeBlanc[1], R. Maingi[1], C.K. Phillips[1], L. Roquemore[1], P.M. Ryan[2], S. Sabbagh[3], G. Taylor[1], K. Tritz[4], J.R. Wilson[1], S. Zweben[1]

[1]*Princeton Plasma Physics Laboratory, Princeton, NJ 08543, USA*

[2]*Oak Ridge National Laboratory, Oak Ridge, TN 37831, USA*

[3]*Columbia University, New York, NY, USA*

[4]*Johns Hopkins University, Baltimore, MD 21218, USA*

Introduction

RF heating deposition spirals are observed on the divertor plates on NSTX as shown in Fig. 1 for a NB plus RF heating case. It has been shown that the RF spiral is tracked quite well by the spiral mapping of the strike points on the divertor plate of magnetic field lines passing in front of the high harmonic fast wave (HHFW) antenna on NSTX [1, 2]. Indeed, both current instrumented tiles and Langmuir probes respond to the spiral when it is positioned over them. In particular, a positive increment in tile current (collection of electrons) is obtained when the spiral is over the tile (Fig. 2). This current can be due to RF rectification [3] and/or RF heating of the scrape off layer (SOL) plasma along the magnetic field lines passing in front of the the HHFW antenna. It is important to determine quantitatively the relative contributions of these processes. Here we explore the properties of the characteristics of probes on the lower divertor plate [4] to determine the likelyhood that the primary cause of the RF heat deposition is RF rectification.

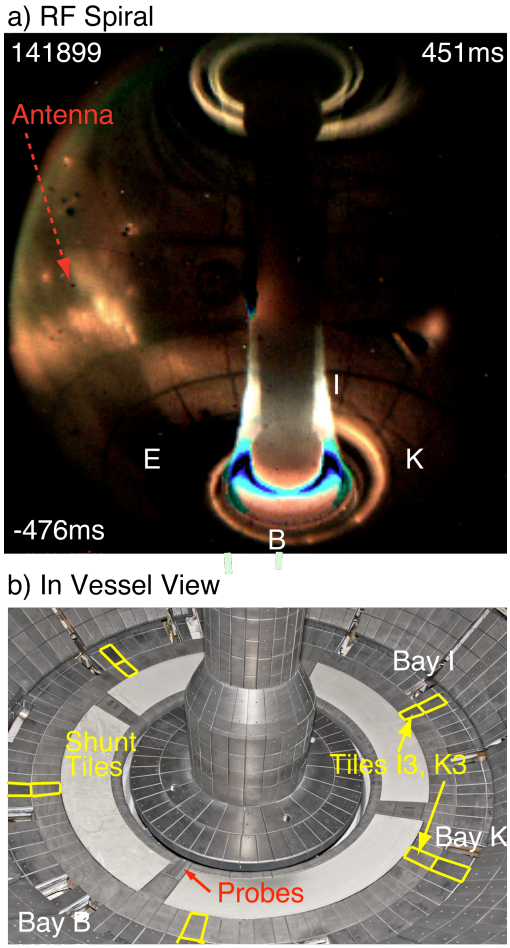

Figure 1. (a) RF deposition spiral for shot 141899 at 0.451 sec with subtraction of background at t = 0.476 sec (after RF pulse). (I_P = 1 MA, B_T = 4.5 kG, P_{RF} = 1.3 MW, P_{NB} = 2 MW.) (b) In vessel view.

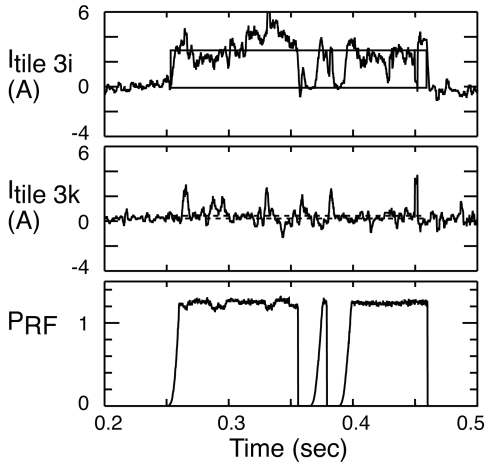

Figure 2. Tile currents for (a) tile 3i under the spiral and (b) tile 3k which is not under the spiral as indicated by the calculated field line strike points on the divertor. P_{RF} vs time is shown in (c) for comparison. (Shot 141899 with parameters given for Fig. 1.)

Probe characteristics for the P_{NB} + P_{RF} case

The floating potentials for probes P2 and P4 at Bay B on NSTX are shown in Fig. 3(a) for the case of Figs. 1 and 2. P4 is under the spiral and V_{fl} exhibits a large negative shift with the application of P_{RF} whereas there is little effect on the V_{fl} for P2 since it is not under the spiral (R = 70.59 cm/64.67 cm for P4/P2 and P2 is inboard of P4 by 5.92cm). Again, this V_{fl} shift can be due to RF rectification and/or plasma heating in the SOL. In Fig. 3(b), it is shown that the P4 current for V_{P4} = 0 (the divertor tile potential) follows quite well the current collected by tile 3i (also in line with the spiral [1]), and is in qualitative agreement with the ratio of the probe surface area to the tile surface area, and the reduction in heat deposition for the spiral at Bay B. $\Delta I_{V=0}$ is positive in both cases indicating electron collection.

In order to determine the relative contributions of SOL heating versus RF rectification, the probe I-V characteristic must be scrutinized carefully. Assuming RF rectification alone is governing the probe response, the magnitude of the shift in floating potential $|\Delta V_{fl}|$ is related to the magnitude of the RF voltage V_{rf} at the probe by [5]

$$\exp(|\Delta V_{fl}|/T_e) = I_0(V_{rf}/T_e), \qquad (1)$$

assuming the probe I-V characteristic remains an exponential curve in the vicinity of V_{fl} and that T_e and I_{sat} are unchanged by the application of the RF voltage. (I_0 is the modified Bessel function.)

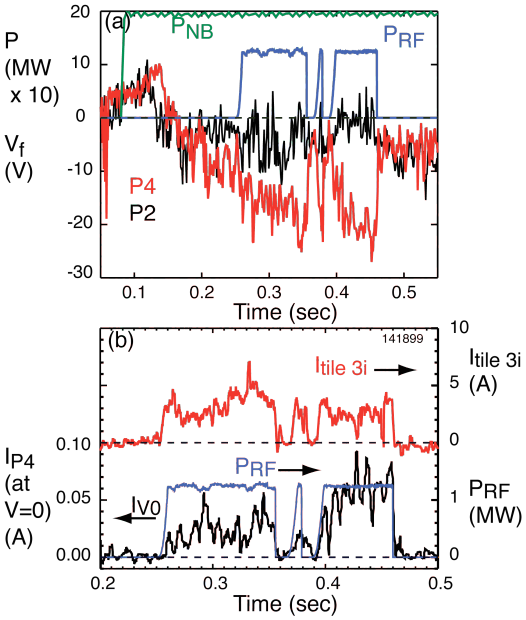

Figure 3. (a) V_{fl} for pobes P4under the spiral and P2 outside the spiral, and (b) comparison of I_{P4} for V_{P4} = 0 to the tile current on tile 3i. (Shot 141899 with parameters given for Fig. 1.)

In Fig. 4, the I-V characteristics for P4 (under the spiral) and P2 (away from the spiral) are compared for t = 0.451 s. Even though the probe current signals are rather noisy in this case due to turbulence at the divertor plate, averaging over 6 consecutive 1 ms probe voltage sweeps give

reasonable characteristics in the vicinity of V_{fl} for comparison. In the vicinity of the floating potentials, relatively good exponential fits are obtained with the same I_{sat} (15 mA) and T_e (13.5 eV), with a shift in the floating potential of $|\Delta V_{fl}| = 24$ V. The T_e value is close to that measured with Thomson scattering at the midplane along the incident field line. $T_{eTS} \sim 10$ eV for $\Delta R_m = 2.1$ cm/1.4 cm from the last closed flux surface (LCFS) for P4/P2. The value of $V_{rf} \sim 44$V is then obtained from Eq. 1.

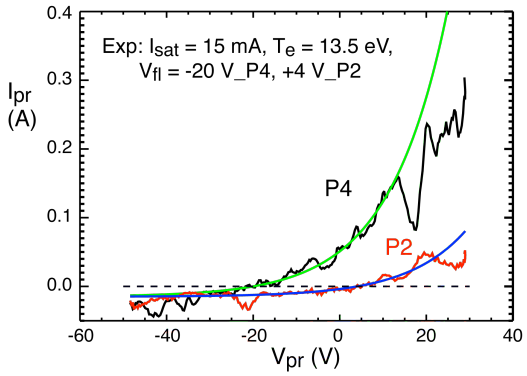

Figure 4. Probe characteristics for P4 under the spiral and P2 away from the spiral for shot 141899 at t = 0.451 s – averaged over 6 consecutive 1 ms voltage sweeps. Exponential fits have same I_{sat} and T_e values, but different V_{fl} values as shown, (Shot 141899 with parameters given for Fig. 1.)

As indicated in Fig. 4, the P4 current deviates from an exponential above a certain voltage (~12V) as expected and the P2 current should then deviate from an exponential at V ~ 12V + V_{rf} ~ 56V. The relatively large level of noise causes the P2 current to undulate above ~ 15V but on average it should approximate the exponential at higher voltages if RF rectification is dominant in this case.

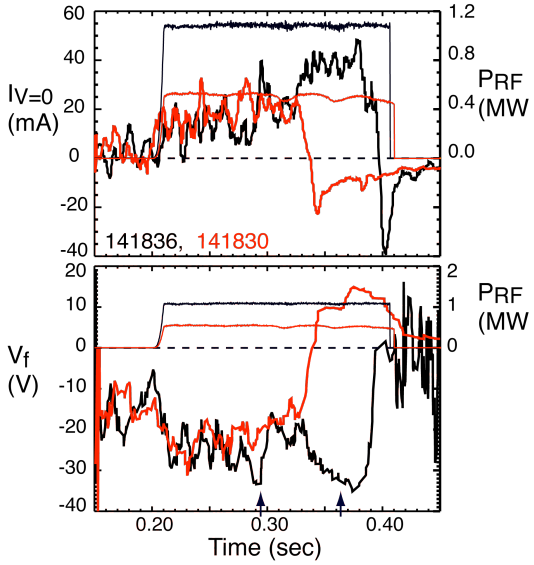

Figure 5. RF spiral effects for P1 for RF only cases at P_{RF} = 1.1 MW and 0.55 MW. (Shots 141836 and 141830, I_P = 0.65 MA, B_T = 5.5 kG, helium.)

Probe characteristics for the P_{RF} only case

The probe current noise level is greatly reduced in the P_{RF} only case and a better comparison between probes with and without the spiral over them can be made. The $I_{V=0}$ and V_{fl} values for P1 (under the spiral at R = 63.82 cm) are shown in Fig. 5 for the two values of P_{RF} = 1.1 MW and 0.55 MW for the conditions shown in the caption. Significant responses to the application of P_{RF} are seen in both cases up to the times at which $I_{V=0}$ and V_{fl} cross through zero as the outer vessel strike radius (OVSR) crosses over the probe [6]. The I-V characteristics for P1 are compared to those of P3 (3.67 cm outboard of P1 and away from the spiral at R = 67.49 cm) in Fig. 6 at P_{RF} = 1.1 MW for (a) t = 0.3628 s and (b) t = 0.294 s, and at P_{RF} = 0.55 MW for (c) t = 0.294 s (again averaged over 6 consecutive 1 ms voltage sweeps). In all three cases of Fig. 6, relative good exponential fits

to both P1 and P3 are obtained with the same I_{sat} and T_e values, and with a negative shift in V_{fl} on P1. (Here the midplane Thomson scattering temperatures are higher at ~ 40 eV to 50 eV in the three cases of Fig. 6.) Associated V_{rf} values from Eq. 1 are (a) 76 V, (b) 64 V, and (c) 33 V. V_{rf} for Fig. 6(a) is perhaps larger than that for Fig. 6(b) since the OVSR is closer to P1 for Fig. 6(a) [2,6] [R_m ~ 0.10 cm for (a) compared with 0.50 cm for (b) relative to the LCFS]. The V_{rf} for Fig. 6(c) would be expected to be $V_{rf}(b)/\sqrt{2}$ = 45 V for the same edge plasma conditions. However, the OVSR is moving outward at different rates for the two power levels (see Fig. 5 and Ref. 6) and thus the edge conditions and the location of P1 relative to the OVSR are different [R_m ~ 0.50 cm for (b) compared with 0.30 cm for (c) relative to the LCFS] .

Conclusions

As shown in Figs. 4 and 6, the probe I-V characteristics support the conclusion that the RF effect at the spiral on the divertor is consistent with RF rectification with little added direct plasma heating. Of course, these results need to be made more definitive on NSTX-U with larger probe voltage sweeps. Also coaxial Langmuir probe connections are planned for NSTX-U to permit the amplitude of V_{rf} at the probe to be measured directly.

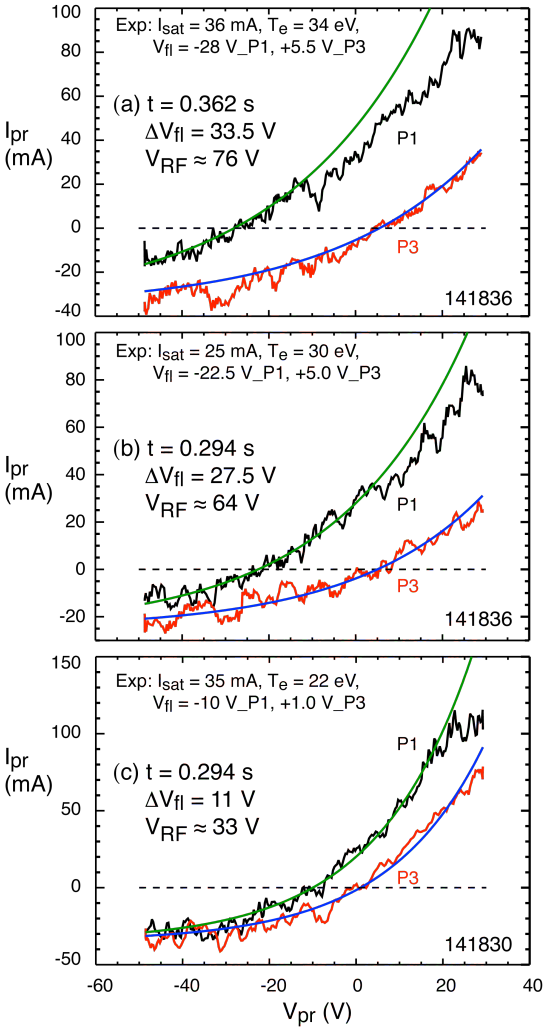

Figure 6. IV characteristics for (a) t = 0.362 s and (b) t = 0.294 s for shot 141836 (P_{RF} ≈ 1.1 MW), and for (c) t = 0.294 s for shot 141830 (P_{RF} ≈ 0.55 MW). Exponential fits for P1 and P3 have the same I_{sat} and T_e for each case, with ΔV_{fl} as noted. (Conditions of Fig. 5.)

References

1. R.J. Perkins *et al., PRL* **109**, 045001 (2012).
2. R.J.Perkins *et al.,* Nuclear Fusion **53** 083025 (2014).
3. K. Takayama, H. Ikegami and S. Miyazaki, *PRL* **5** (1960) 238.
4. J. Kallman *et al., RSI* **81**, 10E117 (2010).
5. A. Boschi and F. Magistrelli, *Il Nuovo Cimento* **29** (1963) 487.
6. J.C. Hosea *et al., RF Conference* (2013, Sorrento), *AIP Conference Proceedings* **1580** (2014) 251.

** This manuscript has been authored by Princeton University under Contract Number DE-AC02-09CH11466 with the U.S. Department of Energy.*